Fibrous TiO$_2$–SiO$_2$ nanocomposite photocatalyst

Ming Jin, Xintong Zhang, Alexei V. Emeline, Zhaoyue Liu, Donald A. Tryk, Taketoshi Murakami and Akira Fujishima*

The electrospinning method is employed to prepare a fibrous TiO$_2$–SiO$_2$ (Ti : Si = 1 : 2) nanocomposite photocatalyst, in which Degussa P25 TiO$_2$ nanoparticles are embedded in the body of SiO$_2$ fibers and which shows good photocatalytic activity due to its 3-D open structure, as evidenced by photocatalytic reduction of silver ions and decomposition of acetaldehyde.

Fibrous photocatalysts are attractive for practical applications in environmental cleanup. Compared to conventional film photo-catalysts, the fibrous photocatalyst has a greater surface-to-volume ratio and a 3-D open structure that allow its surface active sites to be accessible for reactants more easily and effectively.[1] The special open structure of fibrous photocatalysts also makes it possible to combine an additional filtering function in the same material. Despite these interesting properties, few reports have dealt with fibrous photocatalysts, due to the lack of facile preparation methods. Here, we report a novel method to prepare fibrous TiO$_2$–SiO$_2$ photocatalysts by means of electrospinning.[2,3] The fibrous photocatalyst shows good photocatalytic activity, as evidenced by the photocatalytic reduction of silver ions and the decomposition of acetaldehyde.

The electrospinning technique has been recognized as a versatile and effective method for the preparation of polymer fibers with extremely small diameters.[4] The morphologies of the electrospun fibers depend on the solvent and the solution properties, as well as other process parameters.[5] Electrospinning combined with thermal decomposition of polymers has also been used to prepare inorganic and composite nanofibers, including TiO$_2$ nanofibers.[6,7] However, these TiO$_2$ nanofibers are quite brittle due to their polycrystalline nature and do not appear to be suitable for photocatalytic applications. We consider here another possibility, which is to embed TiO$_2$ nanoparticles (Degussa P25) with high photocatalytic activity[8] into amorphous SiO$_2$ nanofibers so as to improve the mechanical strength of the fibrous photocatalyst.

A typical preparation is described as follows: 1.5 g of Degussa P25 powder (Nippon Aerisol) was dispersed in 25 mL of absolute ethanol with a 750 W ultrasonic homogenizer. Then, 2.5 g of polyvinylpyrrolidone (PVP, Aldrich, 99%, average MW = 1 300 000) was added to the suspension under stirring, followed by a 0.5 h ultrasonic treatment. The suspension obtained (solution A) was stable for several weeks and contained no large aggregated particles, since no precipitate was found after centrifugation for 1 h

Photocatalyst Group, Special Research Laboratory for Optical Science, Kanagawa Academy of Science and Technology, KSP Bldg. East 412, 3-2-1 Sakado, Takatsu-ku, Kawasaki-shi, Kanagawa, 213-0012, Japan. E-mail: fujishima@newkast.or.jp; Fax: +81-44-819-2038; Tel: +81-44-819-2020

at 3000 rpm. A polymeric siloxane solution (solution B) was prepared by co-hydrolysis of tetraethoxysilane (TEOS) and polydimethylsiloxane (PDMS, Aldrich, 99%, average MW = 6000) in the presence of water and HCl under vigorous stirring at 70 °C, with the molar composition: TEOS : PDMS monomer : HCl : H$_2$O : ethanol = 1 : 1 : 0.007 : 2 : 10. Phase separation of PDMS with solvents occurred in the initial stage of the reaction and gradually disappeared after reaction at 70 °C over 7 d because of the polycondensation between the hydroxyl terminal of the PDMS and the TEOS sol. A calculated volume of solution B was added to the solution A under vigorous stirring to reach a Ti : Si ratio of 1 : 2 to prepare the viscous feed solution for the electrospinning. Then, this solution was loaded into a plastic syringe and delivered at a constant flow rate during the electrospinning of the fibers.[6,7] The electrospinning setup is a home-built one, consisting of a high voltage power supply, a syringe pump, a syringe, and an aluminium foil target. By applying a voltage of 20 kV to the flat-tip needle (22 gauge) of the syringe, a jet formed at the end of the needle, and fibrous materials were deposited on glass or conductive glass substrates attached to the aluminium target. The as-prepared fibers were heated to 550 °C at a rate of 10 °C min^{-1} and held at that temperature for 4 h to burn out the organic components and convert the polymeric siloxane into SiO$_2$. The addition of PDMS, a linear polymer, was considered to be important in the formation of robust SiO$_2$ fibers due to the twisting of the PDMS chains during the elevation of the temperature.

SEM measurements (Fig. 1) confirmed the formation of fibrous materials. The unheated fibers showed a diameter range of 700–900 nm and quite a smooth surface, although some protuberances could be found due to the existence of the P25 TiO$_2$ nanoparticles. Calcination at high temperature caused the shrinking of the fibers to a range of 500–700 nm in diameter, with roughening of the fiber surface, and the formation of 'knots' between fibers. The shrinking of fibers upon calcination is a common phenomenon because of the burning off of the organic components. The roughening of the fiber surface is due to the exposure of the TiO$_2$ nanoparticles to the surface after fiber shrinkage. The formation of knots is desirable, since it should enhance the strength of the fibers by forming an interconnected framework. This phenomenon was only observed when PDMS was included in the feed solution. When TEOS alone was used to prepare the polymeric siloxane solution, no knots were observed at the contact points of the fibers. We thus attributed the formation of knots to the melting of PDMS segments during heating. The molecular weight of PDMS was found to influence the formation of knots. PDMS of smaller molecular weight, for example MW 2000, hindered the formation of knots. Higher molecular weight
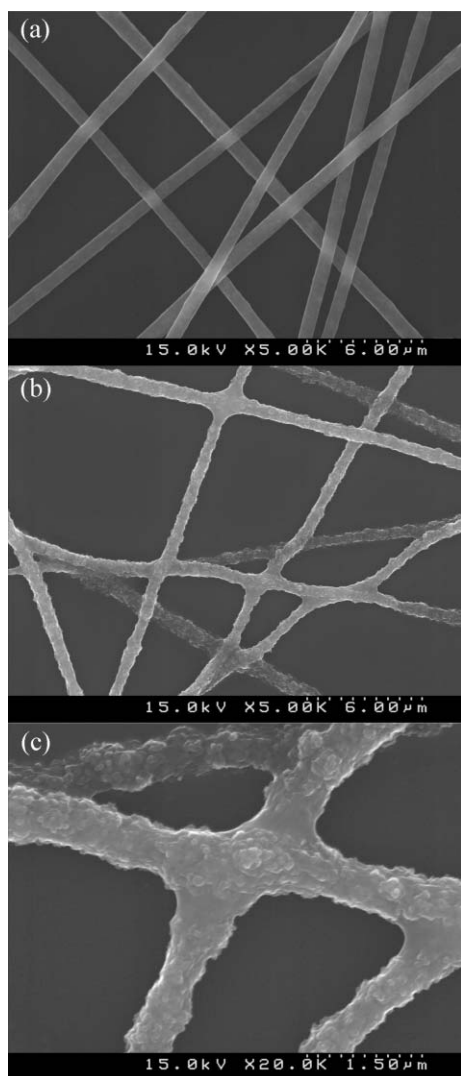
Fig. 1 SEM images of the nanocomposite fibers: (a) before calcination; (b) after calcination at 550 °C for 4 h; and (c) magnified image of (b).

Fig. 2 UV-visible spectra of the Ag-deposited TiO₂–SiO₂ nanocomposite fibers coated on glass slides as a function of irradiation time; the inset shows the change of the color following the irradiation time.

PDMS, for example MW 110 000, however, led to the formation of films instead of a fibrous structure after calcination.

The fibrous TiO₂–SiO₂ photocatalyst showed good activity for photocatalytic reduction of Ag⁺ ions. Glass slides coated with TiO₂–SiO₂ nanocomposite fibers were dipped in an aqueous solution containing 0.1 M AgNO₃ and 10% ethanol solution and were illuminated with UV light of 1 mW cm⁻² ('black light' lamp). The fibrous photocatalyst-covered surface changed color immediately due to the deposition of Ag.[9] The color change was monitored with UV-visible spectroscopy (UV-2450, Shimadzu); the data are shown in Fig. 2. Pure TiO₂–SiO₂ fibers had no absorbance in the visible region. After only 1 min UV illumination, a band appeared at *ca.* 410 nm, corresponding to the surface plasmon resonance band of Ag nanoparticles.[10] This peak exhibits a broad full-width at half-maximum (fwhm) of 100 nm and a tailing effect, which indicate the existence of a broad distribution in size and morphology for these silver nanoparticles.[11] With the prolongation of the illumination time, the maximum absorption of the Ag plasmon band increased and shifted gradually to 460 nm, due to the increasing particle size. After 30 min illumination, the
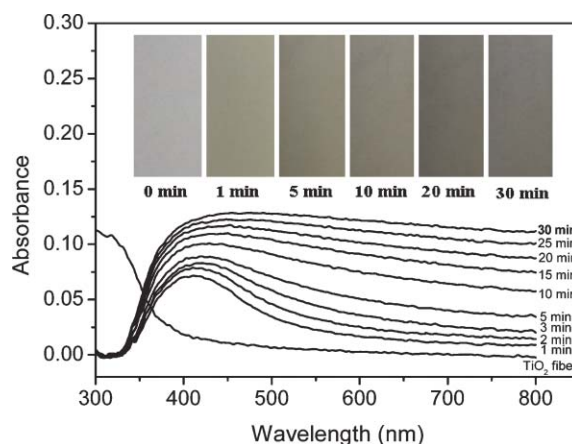
surface turned black, as shown in the images in the inset. Thus, the P25 TiO₂ nanoparticles remained photocatalytically active, even though they were embedded in the body of the SiO₂ fibers.

Further, we investigated the photocatalytic decomposition of acetaldehyde on the fibrous TiO₂–SiO₂ nanocomposite photocatalyst. This was carried out at room temperature. An O₂(20%)–N₂ gas mixture adjusted to a relative humidity of 50% was used to fill the 500 mL Pyrex glass photocatalytic reaction vessel. Then, measured quantities of acetaldehyde (1 vol% in N₂, Takachiho, Japan) were injected into the reactor using a syringe. After equilibrium in the dark for 2 h, the sample was irradiated with UV light with an intensity of 1 mW cm⁻², and the concentrations of CO₂ and acetaldehyde were followed by gas chromatograph (GC-8A, Shimadzu). The sample size was 7 × 7 cm², and the weight of the nanocomposite fibers coated on the glass was 7.0 ± 0.3 mg, containing 2.8 ± 0.1 mg of the relatively pure P25 nanoparticles. A typical result for the photodecomposition of acetaldehyde is shown in Fig. 3a. The concentration of acetaldehyde dropped slightly in the dark but decreased quickly as a function of irradiation time. The decrease in acetaldehyde concentration could be fitted with a first-order kinetic model, which is a common phenomenon in diffusion-controlled photocatalytic processes.[12] At the same time, the concentration of CO₂ increased at a rate of twice that of the decrease in acetaldehyde concentration, indicating the complete mineralization of acetaldehyde on the fibrous photocatalyst under UV illumination. The initial rate for acetaldehyde decomposition on the fibrous TiO₂–SiO₂ photocatalyst was determined to be approximately half of that for the corresponding quantity of pure P25 powder. This is a promising result, considering that SiO₂ blocks part of the active surface area of the TiO₂ particles. We should also note that immobilized TiO₂ always shows lower activity than its powder form.[12]

TiO₂ powder (Degussa P25) by itself cannot be prepared in the form of fibers, but, with the help of a polymeric siloxane, TiO₂ particles can be immobilized in a fibrous network of SiO₂. We consider that the 3-D open structure of the fibrous photocatalyst has a beneficial effect on its activity. By rough estimation, the fibrous structure has a porosity over 80%, which make the diffusion of reactants facile. In addition, the open structure of
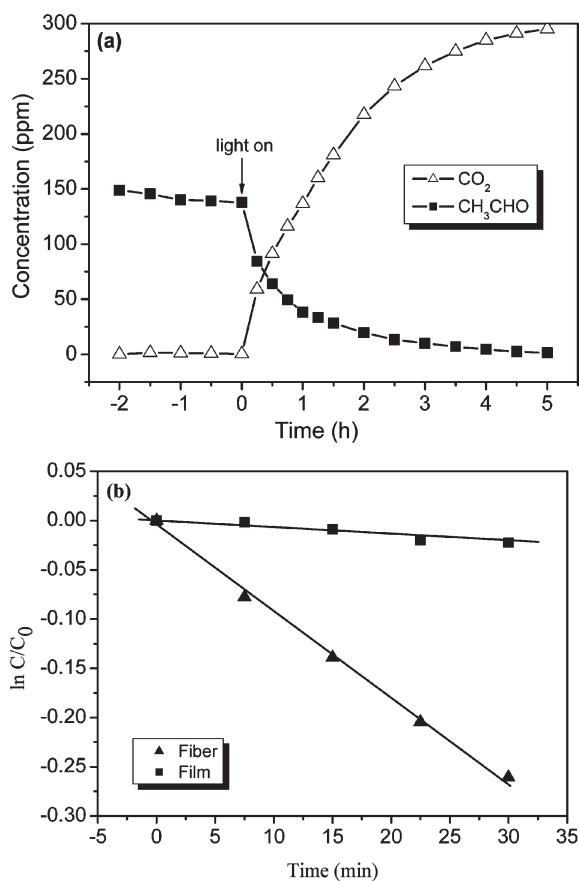
Fig. 3 (a) Curves of acetaldehyde decomposition and CO_2 production as a function of irradiation time in the presence of TiO_2–SiO_2 nanocomposite fibers on a glass slide; the sample area was 50 cm^2, and the light intensity was 1 mW cm^{-2}. (b) Plots of acetaldehyde concentrations *vs.* irradiation time on TiO_2–SiO_2 nanocomposite fibers and composite film coated on glass slides.

the fibrous photocatalyst allows the TiO_2 particles to be exposed effectively to the ambient environment.

In another experiment, we compared thin film and fibrous photocatalysts for acetaldehyde photodecomposition. The thin film, cast from the same precursor solution as that used in the electrospinning and sintered under the same conditions, showed only about one-fifteenth of the rate achieved by the fibers. As shown in Fig. 3b, the thin film showed a rate constant (*k*) of about 0.0006 min^{-1} for acetaldehyde decomposition, while the fibrous photocatalyst showed a rate constant of about 0.009 min^{-1}. A similar comparison was also carried out for TiO_2–SiO_2 nanocomposite fibers with different Ti : Si ratios. It was found that the photocatalytic activity decreased with increasing percentage of Si,

but higher percentages of Ti were detrimental to the strength of the fibers. The Ti : Si ratio of 1 : 2 was the optimum for the present system.

In summary, we have reported a novel route to prepare fibrous TiO_2–SiO_2 nanocomposite photocatalysts *via* the electrospinning technique. This is the first actual report of the successful embedding of TiO_2 (Degussa P25) nanoparticles in SiO_2 fibers for photocatalytic applications. The fibrous photocatalyst has a 3-D open structure which is beneficial for photocatalytic reactions. The interconnected fibrous structure also opens up the opportunity of combining filtering and photocatalytic functions in the same material.

Notes and references

1 S. Madhugiri, B. Sun, P. G. Smirniotis, J. P. Ferraris and K. J. Balkus, Jr., *Microporous Mesoporous Mater.*, 2004, **69**, 77.
2 B. Ding, H. Kim, C. Kim, M. Khil and S. Park, *Nanotechnology*, 2003, **14**, 532.
3 S. S. Choi, B. Chu, S. G. Lee, S. W. Lee, S. S. Im, S. H. Kim and J. K. Park, *J. Sol–Gel Sci. Technol.*, 2004, **30**, 215.
4 D. H. Reneker and I. Chun, *Nanotechnology*, 1996, **7**, 216; Z. M. Huang, Y. Z. Zhang, M. Kotaki and S. Ramakrishna, *Compos. Sci. Technol.*, 2003, **63**, 2223.
5 J. M. Deitzel, J. Kleinmeyer, D. Harris and N. C. B. Tan, *Polymer*, 2001, **42**, 261.
6 B. Ding, C. K. Kim, M. K. Seo and S. J. Park, *Fibers Polymers*, 2004, **5**, 105; D. Li and Y. N. Xia, *Nano Lett.*, 2003, **4**, 555.
7 D. Li and Y. N. Xia, *Adv. Mater.*, 2004, **15**, 1151.
8 D. C. Hurum, A. G. Agrios, K. A. Gray, T. Rajh and M. C. Thurnauer, *J. Phys. Chem. B*, 2003, **107**, 4545; D. C. Hurum, K. A. Gray, T. Rajh and M. C. Thurnauer, *J. Phys. Chem. B*, 2004, **108**, 16483.
9 Y. Ohko, T. Tatsuma, T. Fujii, K. Naoi, C. Niwa, Y. Kubota and A. Fujishima, *Nat. Mater.*, 2003, **2**, 29; K. Naoi, Y. Ohko and T. Tatsuma, *J. Am. Chem. Soc.*, 2004, **126**, 3664.
10 A. S. Kumbhar, M. K. Kinnan and G. Chumanov, *J. Am. Chem. Soc.*, 2005, **127**, 12444; E. A. Hernandez, B. Posada, R. Irizarry and M. E. Castro, *J. Phys. Chem. B*, 2005, **109**, 7251.
11 U. Kreibig and L. Genzel, *Surf. Sci.*, 1985, **156**, 678; C. G. Granqvist and R. A. Buhrman, *J. Appl. Phys.*, 1976, **47**, 2200.
12 I. Sopyan, M. Watanabe, S. Murasawa, K. Hashimoto and A. Fujishima, *J. Photochem. Photobiol., A*, 1996, **98**, 79; Y. Ohko, D. A. Tryk, K. Hashimoto and A. Fujishima, *J. Phys. Chem. B*, 1998, **102**, 2699; A. Fujishima, T. N. Rao and D. A. Tryk, *J. Photochem. Photobiol., C*, 2000, **1**, 1.